Chapter 6

In-silico structural elucidation and mechanism of the purified protein

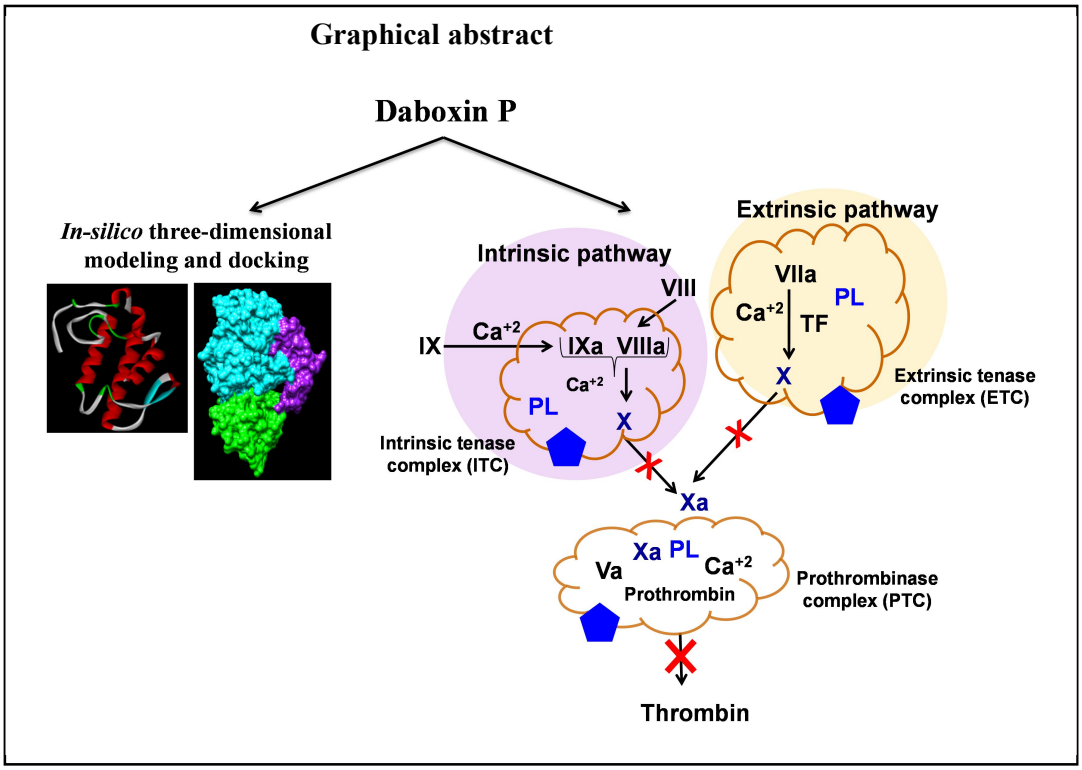

6.1 INTRODUCTION

Snake venom is a rich source of both procoagulant and anticoagulant proteins which can affect the equilibrium of the haemostatic system adversely during envenomation. Consumptive coagulopathy and haemorrhage are some of the most manifested pathological states observed in victims of Russell's viper envenomation (362,363). Paradoxically, these venom components are also bestowed with promising therapeutic potentialities which can be explored to harness the clinical benefits.

In chapter 4 and 5 the purification, biophysical, biochemical and biological characterization of a major anticoagulant protein, daboxin P was discussed. It was found to be non-cytotoxic to the tested normal and cancerous mammalian cell lines and exhibited anticoagulant activity under *in-vitro* and *in-vivo* conditions. It delayed the coagulation time of extrinsic and intrinsic pathway but did not affect the thrombin time and was devoid of fibrinogenolytic activity. This suggests its anticoagulant effect upstream of the common pathway. Considering this prospective, the objective of the present study is to understand the anticoagulant mechanism of this major protein from the venom of Indian *Daboia russelii*.

6.2 MATERIALS

Serine proteases: FXIIa was bought from Merck Calbiochem (Darmstadt, Germany) while FXIa, FIXa, VIIa, FX, FXa and thrombin were purchased from Haematological Technologies Inc. (Vermont, USA). On the other hand, inactivated form of serine protease, FVIII and Tissue factor Innovin were obtained from Creative Biomart (New York, USA) and Siemens (Murburg, Germany) respectively.

Chromogenic substrates: S-2366 (pyroGlu-Pro-Arg-pNA•HCl), S-2302 (H-D-Pro-Phe-Arg-pNA•2HCl), S-2222 (Bz-IIe-Glu (γ-OR)-Gly-Arg-pNA•HCl), S-2765 (Z-D-Arg-Gly-Arg-pNA•2HCl), S-2238 (H-D-Phe-Pip-Arg-pNA•2HCl) and S-2288 (H-D-Ile-Pro-Arg-pNA•2HCl) were procured from Chromogenix (New Jersey, USA) while spectrozyme ($MeSO_2$-D-CHG-Gly-Arg-pNA.AcOH) was purchased from Sekisui Diagnostics (Massachusetts, USA).

Others: The stypven time reagent, RVV-X was procured from Haematological Technologies Inc. (Vermont, USA) and the phospholipid blend of phosphatidylcholine and phosphatidylserine (DOPC:DOPS) was obtained from Avanti Polar Lipids Inc. (Alabama, USA). Variegin was a generous gift from the Protein Science laboratory, Department of Biological Sciences, National University of Singapore. Ethylenediaminetetraacetic acid (EDTA) was bought from Sigma (Missouri, USA).

All other chemicals and reagents used are discussed in the material section of previous chapters.

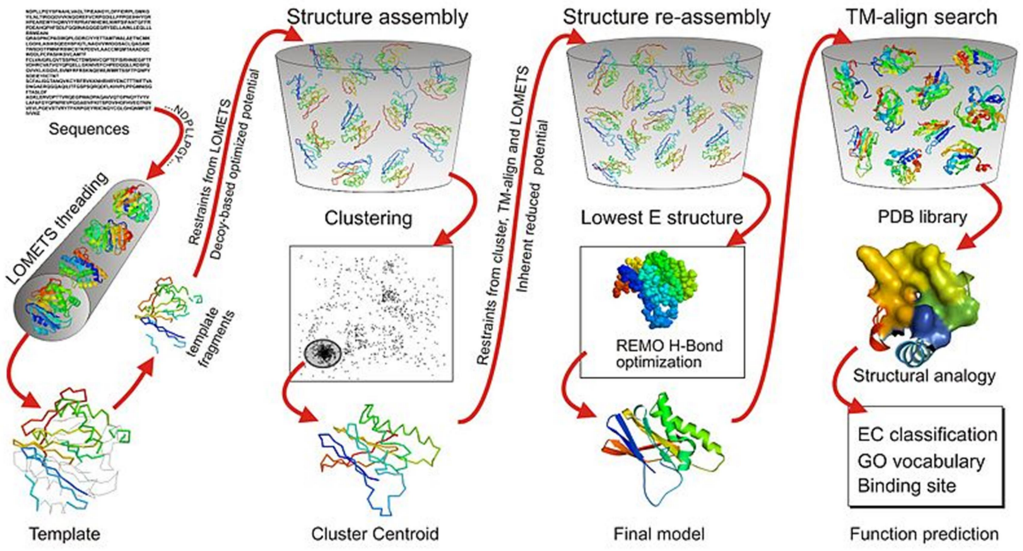

Figure 6.1: **Graphical illustration of the various steps involved in 3D structure modeling of a protein by I-TASSER server. (Adapted from Roy A et. al. Nature Protocols, 2010) (495). 1. Threading:** template proteins sharing sequence similarity with the query are selected from the database using PSI-BLAST. Based on multiple sequence alignment the profile sequence and secondary structures are generated using PSIPRED. The template alignments are generated by threading the secondary structure with the PDB template structures using LOMETS. The predicted template alignment is assessed with the Z-score (expressed as energy score in standard deviation which takes into account the statistical mean of all alignments). **2. Structural assembly:** The aligned templates are fragmented and assembled for structural conformation using *ab initio* modeling and Monte Carlo simulation. **3. Model selection and refinement:** The assembled fragments are simulated again to remove steric hindrance which further refines the global topology of the cluster centroid. The modelled structure with the lowest energy is selected to generate the final structure using REMO (REconstruct atomic MOdel from reduced representation) which produces full atomic protein model based on hydrogen bond optimization (496). **Structure based functional annotation:** The function of the concerned protein is anticipated by comparing its predicted 3D structure with the proteins of the Protein Data Bank. Based on the value of the C-score (value ranges from -5 to 2, a higher score indicates a better modeling) and the TM-score (independent of the protein size and a higher value, ranging from 0 to 1, signifies a better model), the quality of the predicted model is validated.

6.3 METHOD

6.3.1 Three dimensional (3D) molecular modeling of daboin P

For prediction of the *in-silico* tertiary structure of daboxin P, the primary sequence was submitted to online I-TASSER (**I**terative **T**hreading **ASSE**mbly **R**efinement)

server developed by Yang Zhang Lab (http://zhanglab.ccmb.med.umich.edu/I-TASSER/) (495,497,498). A schematic representation of the various steps involved in protein modeling using I-TASSER server has been presented in figure 6.1. Protein structure models are generated by the server considering certain parameters like lowest free energy, C-score (**C**onfidence score), TM-score (**T**emplate **M**odeling score) and RMSD (**R**oot **M**ean **S**quare **D**eviation) value.

6.3.2 Screening for the inhibition of the serine protease activity

In an amidolytic reaction, an activated serine protease cleaves its specific substrate at the amide bond (Arg-pNA) liberating p-nitroaniline which gives a visible colour with an absorbance at 405 nm (Figure 6.2 A). However, in the presence of an inhibitor that binds to its active site, the cleavage of the substrate is prohibited, thus no or little coloured product is generated (Figure 6.2 B).

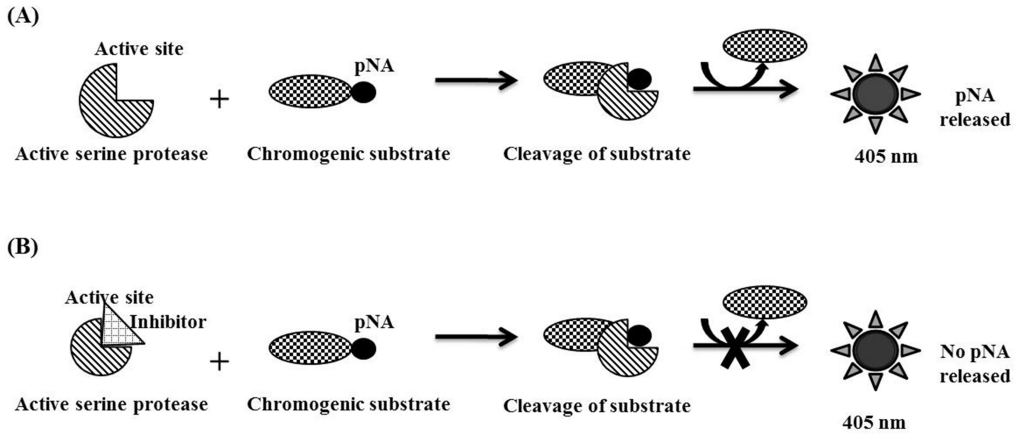

Figure 6.2: Schematic representation of the mechanism underlying the amidolytic activity of the activated serine proteases. (A): Cleavage of the chromogenic substrate by the active serine protease releases pNA which can be quantified at 405 nm. **(B):** In the presence of an inhibitor, which interacts with active site of the protease, the substrate cleavage is prohibited leading to no pNA generation.

The inhibition of amidolytic activity of the activated serine proteases of the extrinsic and intrinsic pathway were screened using their respective chromogenic substrates under *in-vitro* conditions at 37^{o}C. Each of the activated serine proteases FXIIa (60

nM), FXIa (0.125 nM), FIXa (333 nM), FXa (0.43 nM), FVIIa (10 nM), sTF (30 nM) were reconstituted to the desired concentration in the activation buffer (50 mM Tris-Cl, pH 7.4, 1 mg/ml of BSA, 140 mM NaCl and 5 mM $CaCl_2$) and their respective chromogenic substrates viz., S-2302 (1 mM), S-2366 (1 mM), spectrozyme (0.4 mM), S-2765 (0.65 mM) and S-2288 (500 µM) were dissolved in Milli Q water (499).

Briefly, in a reaction volume of 150 µl, each of the reconstituted serine protease was pre-incubated with different concentration of daboxin P (0.01, 0.1 and 1 µM) at 37^{o}C for 5 min. Subsequently, the respective chromogenic substrates were added to each reaction mixtures to initiate the amidolytic reaction. The rate of p-nitroaniline generation upon the cleavage of the substrate was quantified at 405 nm using UV-Vis MultiSkan GO spectrophotometer (Thermoscientific, Massachusetts, USA). Amidolytic activity of the proteases in the absence of daboxin P was considered as 100%.

6.3.3 Effect of daboxin P on the extrinsic tenase complex (ETC)

The extrinsic tenase complex was reconstituted either in presence or absence of phospholipid in activation buffer (50 mM Tris-Cl, pH 7.4, 1 mg/ml of BSA, 140 mM NaCl and 5 mM $CaCl_2$ dissolved in Milli Q water). Briefly, 5 nM of FVIIa was pre-incubated with 10X Innovin (tissue factor, thromboplastin and Ca^{2+} ions) for 15 min at 37^{o}C in activation buffer containing 67 µM of phospholipid vesicles (DOPC:DOPS 7:3) (353).

For preparation of ETC without phospholipid, 20 nM of FVIIa was pre-incubated with 60 nM of soluble tissue factor, sTF for 15 min at 37^{o}C in the activation buffer.

Following this, different concentration of daboxin P (0.01, 0.1, 1 and 3 µM) were added to both the above experiments and incubated for 15 min. Subsequently, 30 nM of FX was added to all the reactions and incubated for 15 min. The reactions were stopped by addition of quenching buffer (50 mM Tris-Cl, pH 7.4, 1 mg/ml of BSA, 140 mM NaCl and 50 mM EDTA in Milli Q water). Finally, 500 µM of S-2222 was added and the rate of FXa generation was quantified at 405 nm using UV-Vis MultiSkan GO spectrophotometer.

6.3.4 Effect of daboxin P on the intrinsic tenase complex (ITC)

The intrinsic tenase complex was reconstituted either in presence or absence of phospholipids. Briefly, of 3 nM of FVIII was pre-incubated with 500 pM of thrombin (FVIII activator) for 10 min at 37^{o}C in the presence of 67 µM of phospholipid vesicles (DOPC:DOPS 7:3) in the activation buffer for the preparation of FVIIIa (500,501). To deactivate the thrombin 10 nM of variegin, a novel thrombin inhibitor, isolated from tropical bont tick (*Amblyomma variegatum*) was added (502). To this mixture, 1 nM of FIXa was added and incubated for 10 min and subsequently different concentrations of daboxin P (0.01, 0.1, 1 and 3 µM) were added. After incubating for 15 min, 25 nM of FX was added and incubated for 15 min.

For reconstituting ITC without phospholipid, the protocol developed by Zhang Y and co-workers with slight modifications was followed (500). Briefly, in a reaction volume of 150 µl, 40 nM FVIII was pre-incubated with 4 nM of thrombin for 10 min at 37^{o}C. Subsequently, the thrombin was deactivated by 40 nM of variegin (incubated for 10 min) followed by addition of 10 nM of FIXa and incubated for 10 min. Following this, different concentrations of daboxin P (0.01, 0.1, 1 and 3 µM) were added and incubated for 15 min. Finally, 1 µM of FX was added and incubated for 15 min.

The reactions in both the experiments were terminated by addition of quenching buffer. Finally, the chromogenic substrate S-2222 (500 µM) was added and the rate of FXa generated was quantified at 405 nm using UV-Vis MultiSkan GO spectrophotometer.

6.3.5 Determination of the inhibitory concentration (IC50) of daboxin P for the extrinsic and intrinsic tenase complex

Briefly, different concentrations of daboxin P were pre-incubated with the reconstituted extrinsic and intrinsic tenase complexes as described in the section 6.3.3 and 6.3.4 in the presence of phospholipids vesicles in the activation buffer. The IC_{50} curve was generated by non-linear curve fit using the software, Origin (OriginLab).

6.3.6 Effect of daboxin P on the prothrombinase complex

The prothrombinase complex was reconstituted by pre-incubating 10 pM of FXa with 1 nM of FVa for 15 min. After reconstitution, different concentration of daboxin P were added and incubated for 15 min.

In another set of experiment, 10 pM of FXa was pre-incubated with different concentrations of daboxin P for 15 min followed by addition of 1 nM of FVa. Subsequently, 12.5 nM of prothrombin was added and the reaction mixture was incubated for another 15 min (346).

The reactions were stopped by addition of quenching buffer (50 mM Tris-Cl, pH 7.4, 1 mg/ml of BSA, 140 mM NaCl and 50 mM EDTA in Milli Q water). Finally, 250 μM of chromogenic substrate S-2238 was added and the amount of thrombin generated was quantified at 405 nm using UV-Vis MultiSkan GO spectrophotometer.

6.3.7 Fluorescence emission spectroscopy

The physical interaction of daboxin P with the activated and the inactivated form of the coagulation FX was determined by fluorescence emission spectroscopy. Briefly, daboxin P (1 μM) was pre-incubated for different time (10 min & 20 min) with FX (0.05 μM) or FXa (0.1 μM) in 20 mM Tris-Cl, pH 7.4. The incubation was carried out both in the presence and absence of $CaCl_2$ (5 mM). The emission spectra of the individual components, daboxin P, FX and FXa and the mixtures (FX-daboxin P and FXa-daboxin P) were recorded from 200 to 500 nm with an excitation wavelength of 280 nm at room temperature using a quartz cuvette (1 cm path length) on fluorescence emission spectrophotometer (LS 55, Perkin Elmer, Palo Alto, CA). The emission spectra of the mixtures were compared with that of the spectra of the individual components to observe for any changes in the fluorescence emission after incubation.

6.3.8 Cyanogen bromide activated sepharose affinity chromatography

Briefly, 0.1 g of CNBr activated resin was swollen overnight in 12.5 ml of ice cold 1 mM HCl (HCl maintains the integrity of the reactive groups of the resin) at 4^oC. Next day, the resin was washed with 5 column volume (CV) of distilled water followed by 5 CV of coupling buffer (0.1 M $NaHCO_3$ and 0.5 NaCl, pH 8.3-8.5). Daboxin P (40

µg) was added to the matrix and incubated for 6 h at room temperature with gentle swirling. The matrix was washed with coupling buffer twice to remove any unbound daboxin P molecules. Consequently, the matrix was incubated with 0.2 M glycine (freshly prepared) for 2 h with mild swirling. Subsequently, the matrix was alternatively washed with acidic (0.1 M acetate buffer, pH 4.0) and basic buffer (coupling buffer) for 5 times to remove the blocking solution. After thorough wash, 8 µg of FX or FXa were added to the matrix and incubated for 1 h at room temperature with mild shaking. The unbound FX or FXa molecules were removed by extensive wash with coupling buffer for 2 CV. Finally, elution of FX or FXa was carried out with elution buffer (20 mM HCl + 1M NaCl).

The elution of bound FX and FXa was confirmed by 12.5% glycine SDS-PAGE under non-reduced condition as described in section 2.3.2 of Chapter 2 and stained using Pierce™ silver staining kit, Life Technologies (Thermo Fischer Scientific, Massachusetts, USA).

6.3.9 Molecular docking of daboxin P

The 3D model of daboxin P and the crystal structure of FXa (PDB: 2BOH) were further equilibrated by molecular dynamic simulation using ff99SB force field of AMBER 12 (**A**ssisted **M**odel **B**uilding with **E**nergy **R**efinement) (503). The molecular docking between the equilibrated structures was performed using PatchDock server (http://bioinfo3d.cs.tau.ac.il/PatchDock/) considering FXa as the receptor and daboxin P as the ligand. PatchDock uses geometry based shape complementarity and generates models with large interface surfaces and least steric hindrance (504,505). The generated candidate solutions are validated based on score function which takes into account the geometry fit, atomic desolvation energy and RMSD clustering (4 Å) (506). The conformer of daboxin P and FXa with the highest atomic contact energy (ACE), score and interface surface area was selected for further refinement by Firedock server (http://bioinfo3d.cs.tau.ac.il/FireDock/) which readjust the interface side chains and relative alignment of the conformer molecules based on global free energy ranking (507,508).

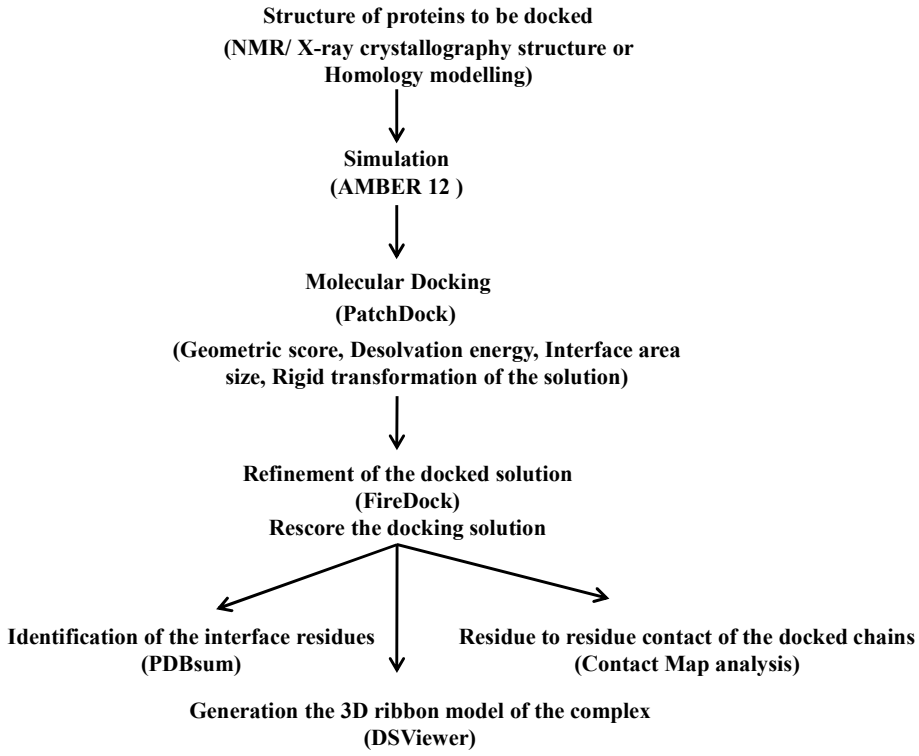

Figure 6.3: Flowchart showing the various steps involved in molecular docking to understand protein-protein interaction.

A flow chart showing the various steps involved in protein docking has been shown in figure 6.3. The ribbon and solvent accessible surface charge model of the docked solution of daboxin P and FXa was generated using DS ViewerPro 5.0 (Accelrys Inc).

The interface amino acids residues and the type of interactions of the selected conformer of the docked complex were identified by PDBsum server (509). The interface amino acid residue is defined as the residue whose contact distance from the interacting protein partner is less than 6 Å.

Contact map analysis: The interaction between the chains of FXa and daboxin P were also analyzed by Contact map analysis (CMA) (http://ligin.weizmann.ac.il/cma/) (510). CMA analyses the contacts between the residues of protein chains or within a single chain in a given PDB file. It displays residue to residue contacts for the pair of

amino acid residues involved in the interaction in the form of contact map which provide more concrete evidence of the protein structure than its 3D atomic coordinates. It also provides a detailed overview of the atom to atom contact of the pair of interacting amino acid residues. A contact area threshold above 8Å^2 was considered for identifying the residue-residue contacts between the chains of daboxin P and FXa for the present analysis.

6.4 RESULTS

6.4.1 *In-silico* 3D molecular modeling of daboxin P

Based on the primary sequence, I-TASSER server predicted the probable amino acid residues likely to be involved in forming the secondary structure and solvent accessible regions of daboxin P (Figure 6.4 & 6.5). Considering the Z-score, TM-score and RMSD value derived relative to the threading templates of PDB, the 3D models of daboxin P were generated (Figure 6.6 & 6.7).

Out of the predicted models, the one with the highest C-score and TM-score (C-score: 1.4, TM-score: 0.91 ± 0.06 and RMSD value: 1.7 ± 1.5 Å) was selected for further study. The predicted 3D ribbon model of daboxin P is shown in figure 6.8 A & C.

Daboxin P shares 76.23% sequence similarity with ammodytoxin A (AtxA), a PLA_2 enzyme isolated from the venom of *Vipera ammodytes ammodytes* (Figure 6.9) (304). The modelled structure of daboxin P superimposed with AtxA with a RMSD value of 0.9 Å validated its predicted model (Figure 6.8 B & C). The conserved critical regions and the solvent accessible surface model of daboxin P are shown in figure 6.10 A, B & C respectively.

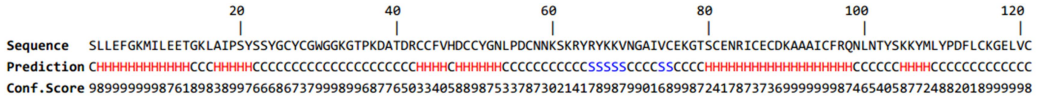

Figure 6.4: Diagram showing the amino acid residues likely to be involved in forming the secondary structure of daboxin P as predicted by I-TASSER server using PSIPRED. H: helix, S: strand, C: coil.

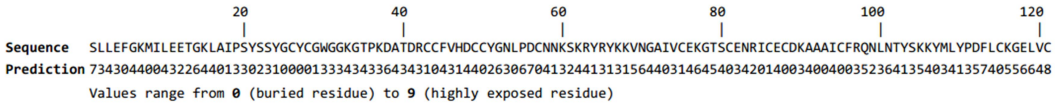

Figure 6.5: Diagram representing the amino acid residues likely to form the solvent accessibility regions of daboxin P as predicted by I-TASSER server.

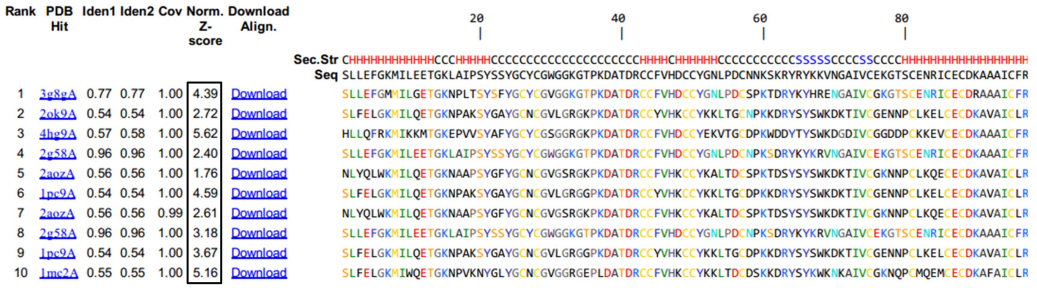

Figure 6.6: Graphical representation of the normalized Z-score of the 10 threading templates for daboxin P used by I-TASSER server.

Rank	PDB Hit	TM-score	RMSD[a]	IDEN[a]	Cov	Alignment
1	4hg9A	0.977	0.68	0.579	1.000	Download
2	1oyfA	0.974	0.69	0.942	1.000	Download
3	1bjiB	0.973	0.71	0.628	1.000	Download
4	1pc9A	0.971	0.76	0.537	1.000	Download
5	1mc2A	0.965	0.84	0.554	1.000	Download
6	2aozA	0.965	0.83	0.562	1.000	Download
7	3r0lD	0.964	0.83	0.603	1.000	Download
8	3g8gA	0.962	0.84	0.760	1.000	Download
9	2ghdB	0.957	0.94	0.628	1.000	Download
10	1db5A	0.956	0.98	0.496	1.000	Download

Figure 6.7: Diagram showing the TM-score and RMSD value of the 10 structural analogs of daboxin P in PDB as determined by I-TASSER.

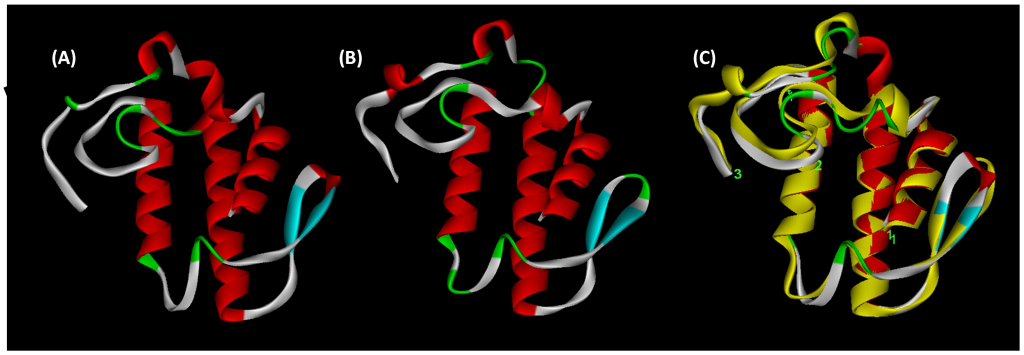

Figure 6.8: 3D molecular modeling of daboxin P. (A): Ribbon model of daboxin P predicted by I-TASSER server. **(B):** Ribbon model of X-ray crystallographic structure of AtxA (PDB 3G8G). **(C):** Superimposed ribbon model of daboxin P (in red, blue, green & white) with AtxA (in yellow) using DS ViewerPro 5.0 (Accelrys Inc.) software.

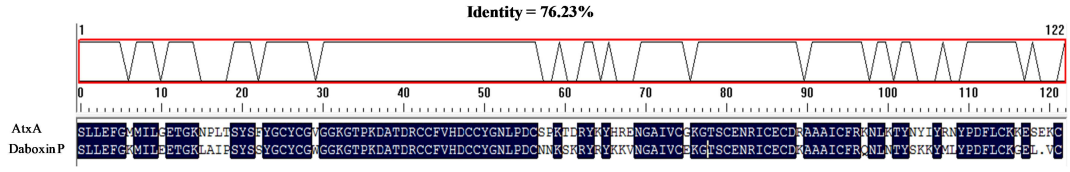

Figure 6.9: Sequence alignment of daboxin P with Ammodytoxin A using DNAMAN 4.1.5.1. (Lynnon BioSoft).

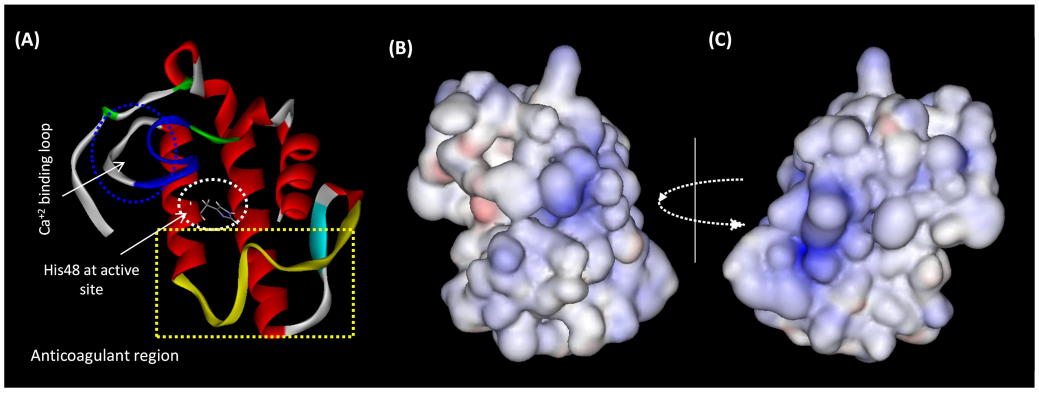

Figure 6.10: Ribbon model with conserved structural conformations and solvent accessible surface of daboxin P generated using DS ViewerPro 5.0. (A): The Ca^{2+} binding loop (YGCYCGCGG) in blue, anticoagulant region (53NLPDCNNKSKRYRYKK68) in yellow and His48 residue is highlighted in stick. **(B & C):** Solvent accessible surface of daboxinP at 180° rotation. The red sections depict regions of lower electrostatic potential (higher electronegativity), blue sections represents region of higher electrostatic potential (lower electronegativity) and white sections show regions without any electrostatic charge.

6.4.2 Screening for serine protease specificity of daboxin P

Daboxin P did not inhibit the amidolytic activity of FXIIa, FXIa, FIXa, FVIIa and FXa when tested using specific chromogenic substrates (Figure 6.11). Although 1 µM of daboxin P could significantly ($P < 0.01$) delay the plasma clotting time of RT, APTT and PT but the same concentration of the protein could not inhibit the amidolytic activity of the tested serine proteases. This suggests that daboxin P does not interact with the active site of these activated serine proteases to exhibit its anticoagulant activity.

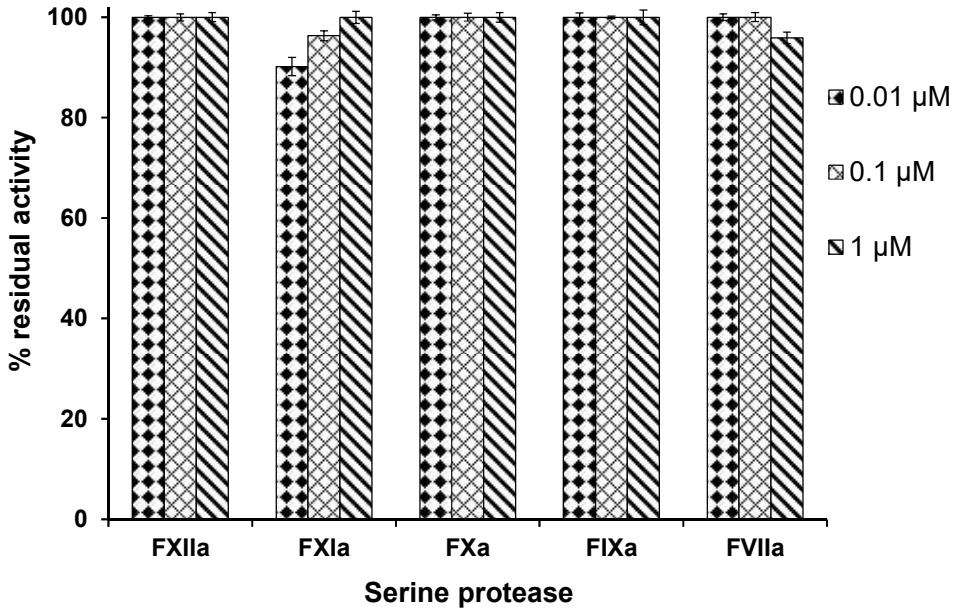

Figure 6.11: Percentage residual amidolytic activity of the activated serine protease pre-incubated with different concentrations of daboxin P. The rate of hydrolysis of the respective substrates was quantified at 405 nm. Activity in the absence of daboxin P was considered as 100%. The results are mean ± SD of three independent experiments.

6.4.3 Effect of daboxin P on the extrinsic tenase complex

Daboxin P inhibited the activation of FX to FXa by the extrinsic tenase complex in the presence of phospholipids in a dose dependent manner (Figure 6.12). Interestingly, daboxin P also inhibited the conversion of FX to FXa in the absence of phospholipids suggesting its anticoagulant activity via non-enzymatic mode, i.e., apart

from phospholipid hydrolysis (Figure 6.12). This was further supported by the inhibitory effect of daboxin P after His48 alkylation. It was observed that the remaining residual activity of 3 μM of daboxin P was lesser in the presence of phospholipids (9.05% ± 1.9) than in its absence (25% ± 2.7) or post alkylation (23% ± 1.8). Furthermore, the residual activity in the absence of phospholipids and post alkylation followed a similar inhibitory pattern especially at 1 and 3 μM which was significantly different from the enzymatic mode.

However, the further increase in concentration did not show much reduction in the activity suggesting a level of saturation in inhibition. The IC_{50} of daboxin P for the extrinsic tenase complex in the presence of phospholipids was found to be 0.43 ± 0.91 nM (Figure 6.13 B).

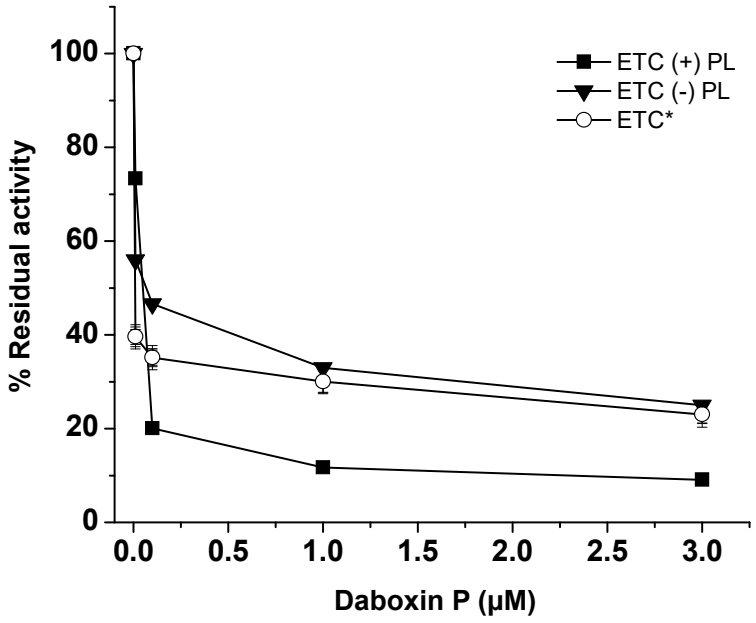

Figure 6.12: Percentage residual activity of the extrinsic tenase complex (ETC) pre-incubated with different concentration of daboxin P. The conversion of FX to FXa was quantified in the presence as well as the absence of phospholipid and with alkylated (His48) daboxin P (indicated by *). The rate of substrate cleavage was measured at 405 nm. The activity of the complex in the absence of daboxin P was considered as 100%. The results are mean ± SD of three independent experiments.

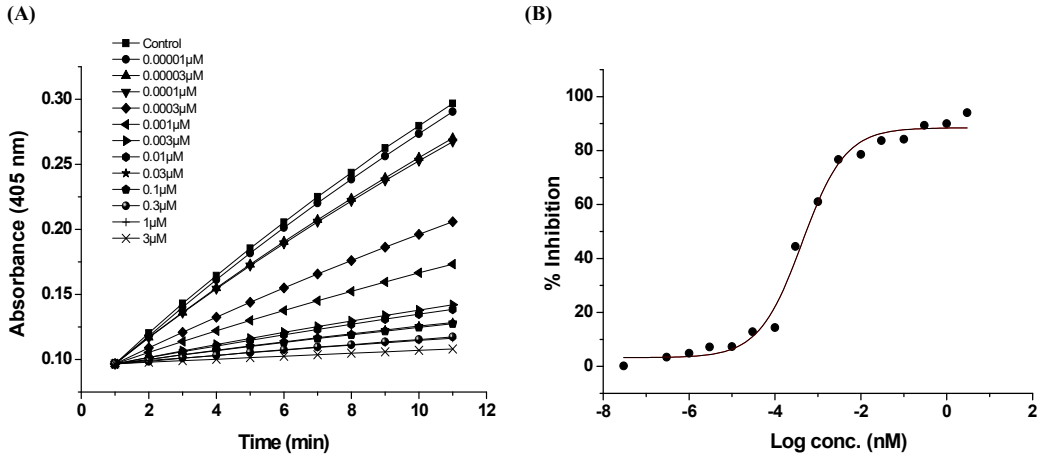

Figure 6.13: IC50 curve of daboxin P for extrinsic tenase complex. (**A)** Progress curves of extrinsic tenase complex pre-incubated with different concentrations of daboxin P. **(B):** Inhibition curve (IC50) was generated using Origin (OriginLab).

6.4.4 Effect of daboxin P on the intrinsic tenase complex

Daboxin P inhibited the formation of FXa by the intrinsic tenase complex both in the presence and absence of phospholipids as well as post-alkylation. This suggests both enzymatic and non-enzymatic mode of anticoagulant mechanism. Daboxin P (3 μM) displayed less percentage residual activity (2.8% ± 1.6) in the presence of phospholipids then in its absence (20.05% ± 2.3) or post alkylation (19.03% ± 1.8) (Figure 6.14). Moreover, the inhibitory effect was more significant till 0.1 μM beyond which there was a gradual saturation in inhibition for all the three experimental conditions. The non-enzymatic mode of action (in the absence of phospholipids or post alkylation) followed a similar inhibitory effect unlike the enzymatic mode (in the presence of phospholipids). The IC_{50} of daboxin P for intrinsic tenase complex was found to be 39.20 ± 1.2 nM (Figure 6.15 B).

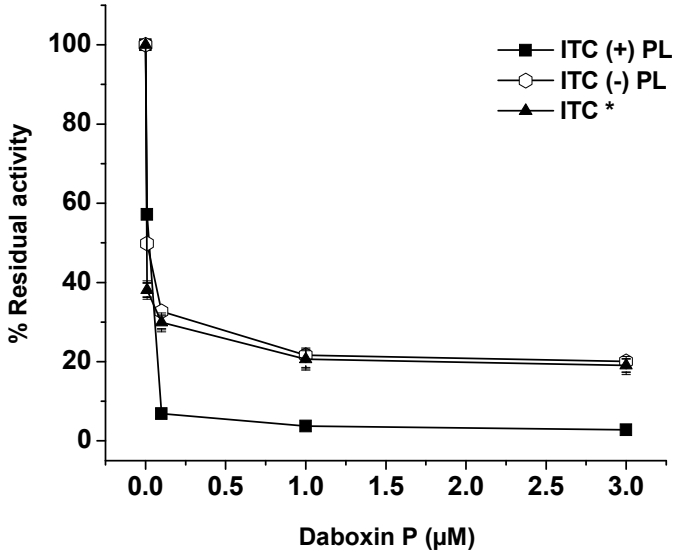

Figure 6.14: Percentage residual activity of the intrinsic tenase complex (ITC) pre-incubated with different concentration of daboxin P. The conversion of FX to FXa was quantified in the presence as well as absence of phospholipid and with alkylated (His48) daboxin P (indicated by *) at 405 nm. The activity of the complex in the absence of daboxin P was considered as 100%. The results are mean ± SD of three independent experiments.

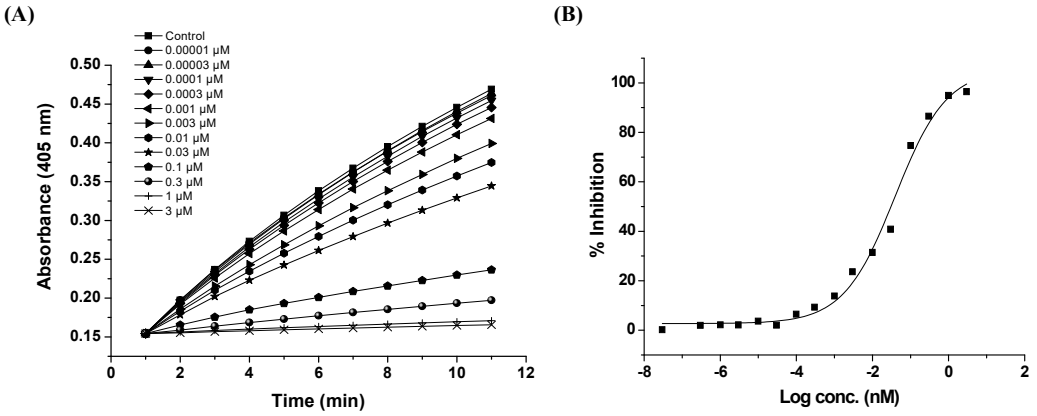

Figure 6.15: IC50 curve of daboxin P for the intrinsic tenase complex. (**A)** Progress curves of intrinsic tenase complex pre-incubated with different concentrations of daboxin P. **(B):** Inhibition curve (IC_{50}) was generated using Origin (OriginLab).

6.4.5 Effect of daboxin P on the prothrombinase complex

Conversion of prothrombin to thrombin by prothrombinase complex was not inhibited when daboxin P was pre-incubated with the complex (FXa-FVa). However, it displayed significant (p-value < 0.001) inhibition in thrombin formation when pre-incubated with FXa (pre-complex) prior to addition of FVa (Figure 6.16). At 3 µM concentration of daboxin P, 90.88 ± 3.2% of residual activity was observed post complex formation while at the same concentration the residual activity was observed to be only 5 ± 2.11% when daboxin P was incubated with FXa prior to prothrombinase complex formation.

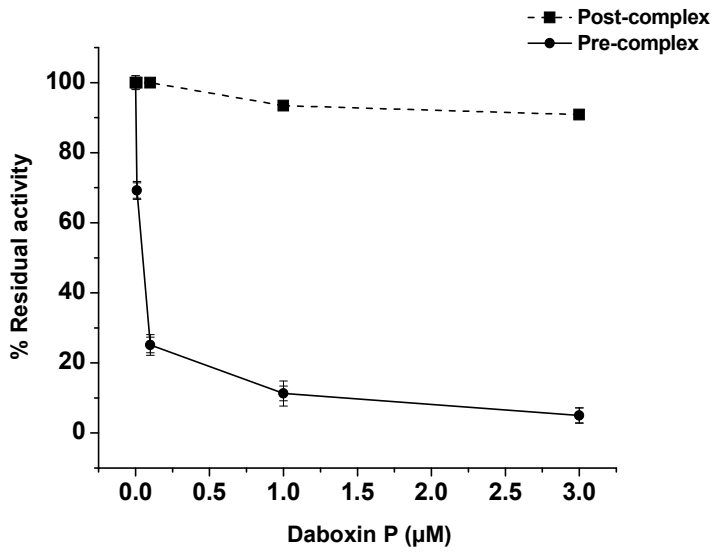

Figure 6.16: Percentage residual activity of the prothrombinase complex (PTC) pre-incubated with different concentration of daboxin P. Different concentrations of daboxin P were either pre-incubated with FXa (pre-complex) followed by FVa or added after the formation of the FXa-FVa complex (post complex). The rate of thrombin generation was quantified at 405 nm. Activity in the absence of daboxin P was considered as 100%. The results are mean ± SD of three independent experiments.

6.4.6 Fluorescence emission spectroscopy

The fluorescence emission intensity of both FX and FXa were gradually decreased in the presence of daboxin P with increasing incubation time. The emission spectra of the mixtures (daboxin P-FX or daboxin P-FXa) were lower compared to the emission

spectra of individual FX or FXa (Figure 6.17). However, the presence or absence of Ca^{2+} ions did not show any effect on the emission spectra of the incubated mixture. This indicates the lack of any effect of Ca^{2+} ions in the complex formation.

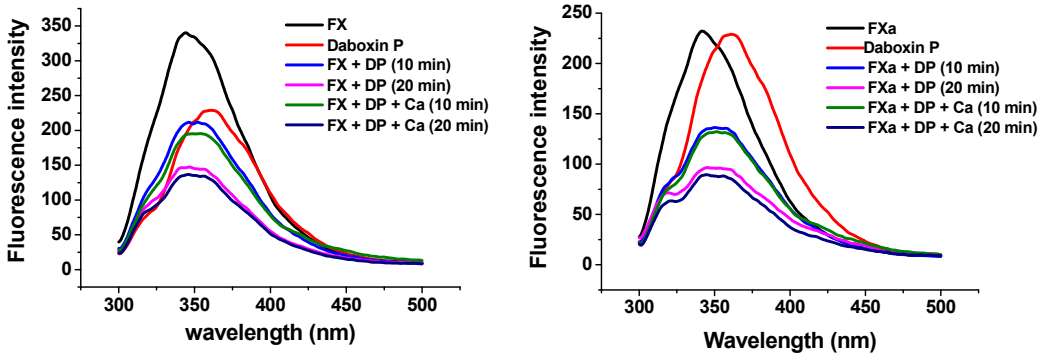

Figure 6.17: Fluorescence emission spectra of daboxin P, FX, FXa and the complex (FX-daboxin P or FXa-daboxin P). Emission spectra of **(A):** FX, daboxin P and FX-daboxin P. **(B):** FXa, daboxin P and FXa-daboxin P for different time intervals at room temperature in presence or absence of Ca^{2+} ions.

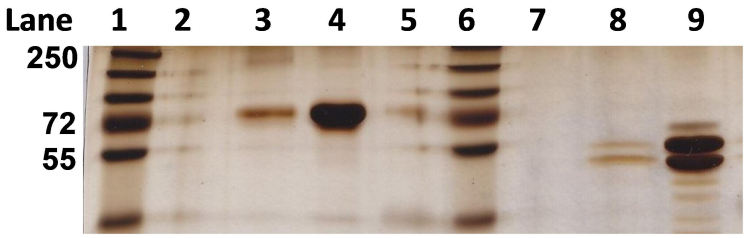

Figure 6.18: 12.5% Glycine SDS-PAGE profile of the fractions of affinity chromatography. Lane 1: PageRuler^{TM} plus pre-stained protein ladder (250-10 kDa), **Lane 2:** flow through (FX), **Lane 3:** FX after elution with 1.0 M NaCl, **Lane 4:** Control (FX), **Lane 5:** blank, **Lane 6:** PageRuler^{TM} plus pre-stained protein ladder (250-10 kDa), **Lane 7:** flow through (FX), **Lane 8:** FXa after elution with 1.0 M NaCl, **Lane 9:** Control (FXa).

6.4.7 Affinity column chromatography

The interaction of daboxin P with FX and FXa was further supported by affinity column chromatography (Figure 6.18). The electrophoretic profile of the flow through of affinity chromatography did not show any protein bands of FX and FXa on the SDS-PAGE gel. However, prominent protein bands were observed between 72 -55

kDa (lane 3) and below 55 kDa (lane 8) under non-reduced state in the eluents when eluted with buffer containing 1 M NaCl.

6.4.8 Molecular docking

The docked complex of daboxin P and FXa with lowest free energy and highest surface contact area generated by PatchDock server was selected for analysing the protein-protein interaction. The docked complex displayed a geometric shape complementarity score of 12234 which refers to a good molecular shape complementarity between the docked chains due to optimal fit with wide interface areas and minimum steric hindrance (504). The interface area of the complex was observed to be 1837 $Å^2$ and atomic contact energy was 472.62 kcal/mol. PDBsum determined seven amino acid residues of heavy chain of FXa to be involved in interaction with eight amino acid residues of daboxin P via hydrogen bonds and non-bonded contacts (Figure 6.19 A & B).

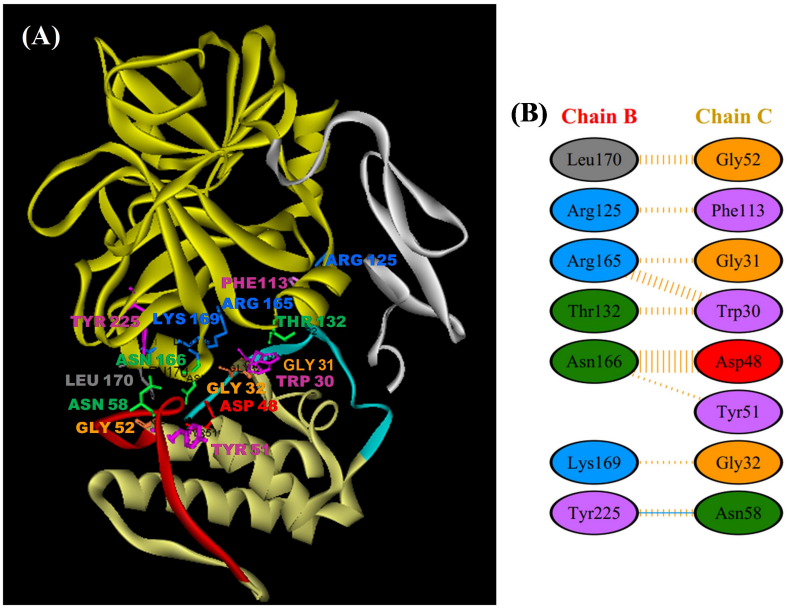

Figure 6.19: ***In-silico*** **molecular docking of daboxin P with FXa. (A):** 3D modeling of FXa and daboxin P generated using PatchDock server. The interface amino acid residues involved in the interaction in daboxin P (Trp30, Gly31, Gly32, Asp48, Tyr51, Gly52, Asn58 and Phe113) and FXa (Thr132, Arg165, Lys169, Asn166, Leu170, Tyr225 and Arg125) are represented in scaled ball and stick. **(B):** Schematic representation of the residues from each chain involved in the interaction as predicted by PDBsum. Blue line indicates hydrogen bond and orange line indicates non-bonded contacts.

The interaction involved 31 interface residues with an interface area of ~500 $Å^2$ from each monomeric chain. The heavy chain of FXa was found to interact with the Ca^{2+} binding loop, helix C, anticoagulant region and C-terminal region of daboxin P (Figure 6.19 and Table 6.1). The interface plot statistics of the complex is summarized in table 6.2.

Table 6.1: Summary of amino acid residues involved in interaction of daboxin P and FXa based on PDBsum analysis.

	Daboxin P	FXa
Interacting residues	Trp30, Gly31, Gly32 (Ca^{2+} binding loop)	Thr132, Arg165, Lys169 (Heavy chain)
	Asp48, Tyr51, Gly52 (Helix C)	Asn166,Lys169,Leu170 (Heavy chain)
	Asn58 (Anticoagulant region)	Tyr225(Heavy chain)
	Phe113 (C-terminal region)	Arg125(Heavy chain)

Table 6.2: Interface statistics of the docked complex of daboxin P and FXa.

Chain	No. of interface residues	Interface area ($Å^2$)	No. of salt bridges	No. of disulphide bonds	No. of hydrogen bonds	No. of non-bonded contacts
B	7	550	-	-	1	31
C	8	550				

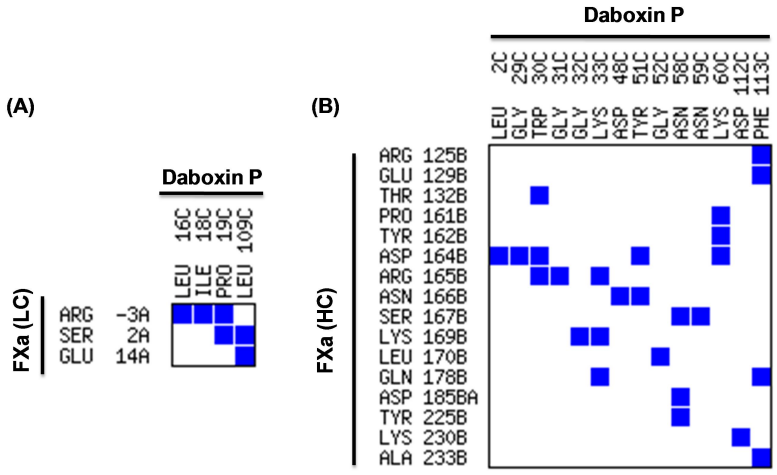

Figure 6.20: Contact map analysis of daboxin P-FXa. Residue to residue contact of daboxin P with **(A):** light chain of FXa and **(B):** heavy chain of FXa. A threshold of 8$Å^2$ contact area has been considered for the analysis.

Contact map analysis: Contact map analysis shows the interaction of both the heavy and light chains of FXa with daboxin P (Figure 6.20). The residues of helix B (Leu16, Ile18, Pro19) and C-terminal region (Leu109) of daboxin P were found to share a contact area greater than the threshold limit (> 8Å^2) with three residues of light chain of FXa (Arg3, Ser2, Glu14) (Figure 6.20 A). On the other hand, fourteen residues of daboxin P namely Leu2 from helix A, Gly29, Trp30, Gly31, Gly32, Lys33 from the Ca^{2+} binding loop, Asp48, Tyr51, Gly52 from the helix C, Asn58, Asn59, Lys60 from the anticoagulant region and Asp112, Phe113 from the C-terminal region were found to share a contact area >8Å^2 with sixteen residues of the heavy chain of FXa (Arg125B, Glu129B, Thr132B, Pro161B, Tyr162B, Asp164B, Arg165B, Asn166B, Ser167B, Lys169B, Leu170B, Gln178B, Asp185B, Tyr225B, Lys230B, Ala233B) (Figure 6.20 B).

6.5 DISCUSSION

The haemostatic system of vertebrates is tightly regulated by a delicate balance between clot formation upon injury and its dissolution to restore normal blood flow. Thrombosis is one of the most severe pathological conditions of the haemostatic system which impedes the flow of blood through the blood vessels forming unwanted blood clots. This leads to the formation of thrombus (static blood clot in vein) or thromboembolus (blood clot in vein that travels from one site to other) (155). This causes some of the most fatal medical conditions like hypoxia (shortage of oxygen supply to the cells and tissues), anoxia (complete cessation of oxygen supply to the tissues or organs) and infarction (necrosis of tissues due to inadequate supply of oxygen) thus, damaging vital organs of the patient. Deep vein thrombosis, pulmonary embolism, myocardial infarction and ischemic stroke are some of the most prevailing medical conditions suffered around the globe owing to the present-day lifestyle (www.coaguchek.com). Such medical complications are mostly dealt by administration of anticoagulant drugs like low molecular weight heparin and its derivatives, vitamin K antagonists as well as NOAC (New Oral Anticoagulants) (511-515). However, these drugs are often accompanied by some limitations associated to efficacy and safety along with unforeseen medical complications (516,517). Thus, search for new anticoagulant with least side effects are perused across the globe.

The venom of snakes and the saliva of haematophagous organisms (leech, hookworm, ticks, etc.) are a rich source of anticoagulant, antiplatelet or antithrombotic components with potent therapeutic application (518). A number of such leads have been already characterized, many of which are queued for clinical trials while some of them are successfully used for treating the patients (502,519-523).

The rich repertoire of pharmacologically active proteins in snake venom are a "Blessings in disguise" with prospective to treat various clinical syndromes like hypertension, thrombosis, haemorrhage etc (524-526). *Daboia russelii* is one such venomous snake with promising therapeutic components. Some of its proteins such as Russell's viper venom X activator (RVV-X) and Russell's viper venom V activator (RVV-V) are being used for various diagnostic assay kits to detect blood coagulation abnormalities in patients and for laboratory purposes. RVV-X, which activates FX to FXa, is used to detect FX deficiency and lupus anticoagulant in plasma. On the other hand, RVV-V, which activates FV to FVa is used to measure the level of FV deficiency and activated protein C level in the plasma.

The present study elucidates the anticoagulant mechanism of a strong anticoagulant PLA_2 enzyme, daboxin P from the venom of Indian *Daboia russelii* (Irula). It delayed the clotting time of plasma both under *in-vitro* and *in-vivo* conditions. Daboxin P delayed the clotting time of RT, PT, APTT and ST but did not exhibit any effect on TT and fibrinogen. This suggests its anticoagulant effect on the extrinsic and intrinsic pathway but not on the common pathway. Based on this observations, the activated serine proteases of the extrinsic and intrinsic pathway were screened to identify the target of daboxin P (527). Screening revealed that it did not inhibit the enzymatic activity of the tested serine proteases of the coagulation cascade. Hence, it might target the complexes of the of the coagulation cascade.

Apart from the individual serine proteases, blood coagulation cascade also comprises of three complexes, viz. extrinsic tenase, intrinsic tenase and the prothrombinase complex which together play a very crucial role in the final fibrin mesh formation. The extrinsic and intrinsic tenase complexes convert the zymogenic FX to its activated form FXa, in the presence of phospholipids and calcium ions. FXa, then

participates in the formation of prothrombinase complex along with FVa, phospholipids and Ca^{2+} ions to convert prothrombin to thrombin. Thrombin then cleaves fibrinogen to fibrin peptides which finally gets cross-linked over the platelet plug to impede blood flow.

It was observed that daboxin P showed profound inhibitory effect on the coagulation complexes when incubated after the complexes were reconstituted. It exhibited dose dependent inhibition of FXa generation by both the Xase complexes in the presence of phospholipids indicating the enzymatic hydrolysis of phospholipid matrix to execute anticoagulation. Moreover, daboxin P also inhibited FXa formation by the Xase complexes in the absence of phospholipids suggesting non-enzymatic mode of action by protein-protein interaction. The display of inhibitory effect by the alkylated (His48) form of daboxin P, further emphasized its non-enzymatic action. Notable observation is that, FX is common for both the Xase complexes apart from phospholipids and calcium ions. Hence, it was hypothesized that daboxin P might interact with FX of the two Xase complexes to exhibit its anticoagulant activity in a non-enzymatic manner. Nonetheless, daboxin P did not inhibit thrombin generation by the prothrombinase complex of the common pathway when incubated with the pre-formed complex (FXa-FVa). On the contrary, a significant delay in thrombin formation (p-value < 0.001) was observed in a dose dependent manner when it was pre-incubated with FXa followed by FVa addition suggesting that it might be interacting with FXa. The reduction in the fluorescence emission spectrum of FX and FXa with increasing incubation with daboxin P and the elution of FXa and FX from affinity column immobilized with daboxin P at 1 M NaCl, support the hypothesis of protein-protein interaction between daboxin P and FX/FXa for exhibiting the anticoagulant effect.

NAPc2/3/4/5 and AceAP1 isolated from hookworms (*Ancyclostoma sp.*) and Ixolaris from tick (*Ixodes scapularis*) are reported as inhibitors of extrinsic tenase complex (528-530). These proteins inhibit the FXa formation by the complex (FVIIa-TF) by interacting with the heparin binding exosite of FX or FXa (528-530). On the other hand, nitophorin-2 is an intrinsic tenase complex inhibitor, isolated from *Rhodnius prolixus* (kissing bug) (531). It is reported to bind to the Gla domain of FIX thus

interfering its activation by FXIa or interact with FVIIa-TF complex affecting FXa generation (531,532). CM-IV, a strong anticoagulant PLA_2 enzyme (isolated from *Naja nigricollis* venom) inhibits both the extrinsic tenase complex and prothrombinase complex (81,182). The anticoagulant region of CM-IV is reported to share a partial sequence similarity with a region of TF and light chain of FVa thus, predicted to interact with FVIIa and FXa respectively (81,182). However, FVa or TF does not share any sequence similarity with the anticoagulant region of daboxin P suggesting a different anticoagulant mechanism by daboxin P (Figure 6.21).

```
Daboxin P: NLPDCNNKSKRYRYKK
FVa        EMKASKPGWWLL-NTSVGENQRAGMQTPFL
CM-IV:     E-KAGKMGCWPYLTLYKYK
TF:                LIY-TLYYWKSS
```

Figure 6.21: Sequence alignment of the anticoagulant region of daboxin P and CM-IV with a region of FVa and TF using DNAMAN. (Partly adapted from Kini, Toxicon, 2005 (81)).

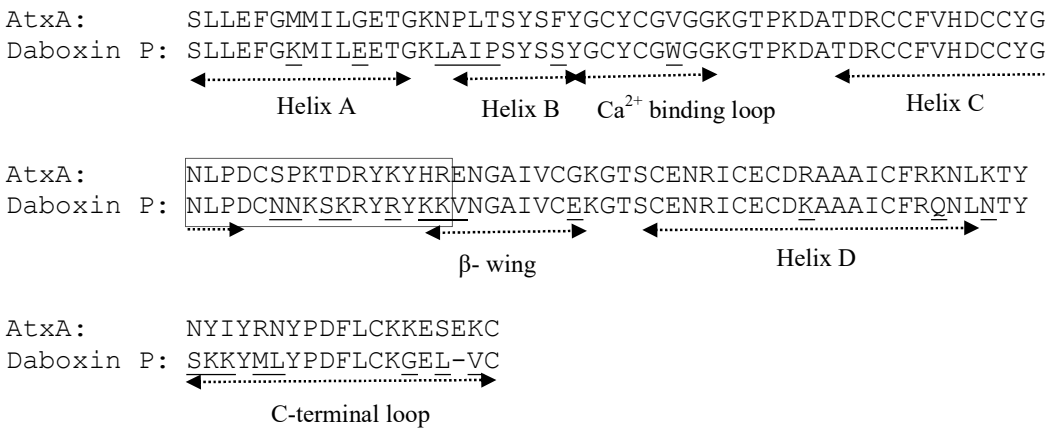

Figure 6.22: Sequence alignment of daboxin P with AtxA along with the conserved secondary structure. The anticoagulant region is shown in box and the amino acid residues varying in daboxin P with respect to AtxA are underlined.

Another PLA_2 enzyme, ammodytoxin A (AtxA), (isolated from *Vipera ammodytes ammodytes* venom) inhibits the activation of prothrombin to thrombin by the prothrombinase complex by binding to FVa binding region on FXa (351). Daboxin P is found to share 76% sequence similarity with AtxA with amino acid substitution at helix A, helix B, Ca^{2+} binding loop, β-wing, helix D and C-terminal region (Figure 6.22). Variations in the primary sequence of snake venom PLA_2 enzymes are well documented in the literature which are known to confer different specificity to these proteins towards diverse pharmacological targets (290).

Molecular docking study performed by Faure and colleagues with AtxA and FXa revealed the interaction of both the heavy and light chain of FXa with AtxA (351). The heavy chain of FXa interacted with the Ca^{2+} binding loop, helix C, β-wing and the C-terminal region of AtxA, while light chain was involved in interaction with the helix A, B and the β-wing of AtxA (351). However, the present molecular docking study revealed the interaction of daboxin P with the heavy chain (chain B) of FXa but not with its light chain. The residues present in the Ca^{2+} binding loop (Trp30, Gly31, Gly32), helix C (Asp48, Tyr 51 and Gly52), anticoagulant region (Asn58) and the C-terminal region (Phe113) of daboxin P were found to be involved in interaction with the heavy chain of FXa (Thr132, Arg165, Lys169, Asn166, Leu170, Tyr225 and Arg125). The amino acid residues of AtxA which were reported to be involved in interaction with the light chain of FXa were found to be substituted in daboxin P (Met7 to Lys7, Asn16 tor Leu16, Pro17 to Ala17, Leu18 to Ile18, Thr19 to Pro19, Arg68 to Lys68). Hence, due to these substitutions daboxin P might not be interacting with light chain of FXa (351). On the other hand, CMA shows the interaction of daboxin P with both the light and heavy chains of FXa. In this analysis, the contact area between the residues is considered but not the distance between the residues as considered in PDBsum analysis. This reveals that the residues of daboxin P which are in close proximity with FXa (heavy and light chain) might hinder the interaction of FXa with its natural co-factors thus, affecting its functioning.

Rudolph and co-workers reported the crucial involvement of Arg165, Lys169 and Lys230 of FXa in forming the core for FVa binding while residues Arg125 and Glu129 were important for the complex formation (533). Thus, interaction of daboxin

P with some of these residues of FXa might create a steric hindrance in forming the FXa-FVa complex hence, inhibiting the prothrombinase complex. Based on site directed mutagenesis and molecular docking, Norledge and colleagues reported that Asp4 and Asp7 of EGF-II of light chain and Asp185a, Lys186 and Lys134 of heavy chain of FXa are crucial for binding to TF/FVIIa complex (534). Present docking study revealed that daboxin P binds to FXa (discussed above) in close vicinity to FVIIa-TF binding region on FX. Hence, it is postulated that interaction of daboxin P with those proximal regions might create a steric hindrance in light chain and heavy chain regions of FX and inhibit the FVIIa-TF or FIXa-FVIIIa formation. The interacting residues involved in FX could not be confirmed by docking analysis as the crystal structure of FX is not available in PDB. Thus, based on the biochemical, biophysical and docking analysis, the present study proposes that daboxin P might interact with both FX and FXa to exhibit its anticoagulant activity.

The probable anticoagulant mechanism of daboxin P can be summed up in the following way. In the presence of daboxin P, the conversion of FX to FXa is inhibited by both the extrinsic and intrinsic tenase complexes. This, in turn, affects the prothrombinase complex which converts prothrombin to thrombin due to the shortage of FXa thus preventing blood coagulation. Simultaneously, FXa formed under physiological condition might interact with daboxin P and inhibit its binding with FVa, which is the co-factor for the formation of the prothrombinase complex. Lack of prothrombinase complex will lead to insufficient thrombin generation which will lead to non-coagulation or delay in clot formation. The probable interactions of daboxin P with the coagulation complexes and FX/FXa is summarized in figure 6.23.

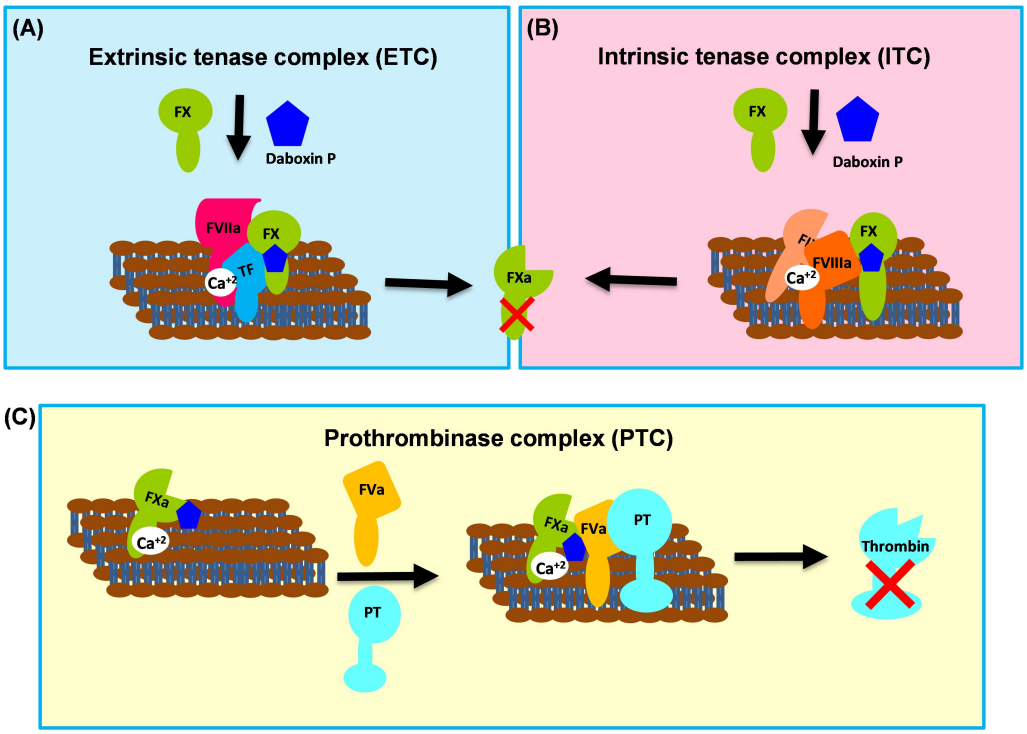

Figure 6.23: The proposed mechanism of interaction of daboxin P with coagulation complexes. (A) & (B): Daboxin P interacts with FX of both the Xase complexes and prevents its conversion to FXa. **(C):** Interaction of daboxin P with FXa of the prothrombinase complex interferes with the binding of FXa with FVa thus inhibiting the conversion of prothrombin to thrombin. The serine proteases of the coagulation cascades, phospholipids and daboxin P are represented in different shapes and colours.

In the present study the anticoagulant mechanism of daboxin P purified from the venom of Indian *Daboia russelii* has been proposed. The biochemical, biophysical and docking studies suggest that daboxin P exhibit anticoagulant mechanism enzymatically by phospholipid hydrolysis and non-enzymatically by targeting FX and FXa. Hence, the current study portrays daboxin P, a major anticoagulant PLA_2 enzyme from the venom of Indian *Daboia russelii* as a natural inhibitor of FX and FXa.